Microchimica Acta (2022) 189: 158
https://doi.org/10.1007/s00604-022-05284-8

ORIGINAL PAPER

# Fluorescence determination of glyphosate based on a DNA-templated copper nanoparticle biosensor

Huajuan Fang[1] · Xingping Zhang[1,2] · Dongxu Gao[1] · Yao Xiao[1] · Liyuan Ma[1] · Hualin Yang[1,3] · Yu Zhou[1,4]

Received: 24 January 2022 / Accepted: 15 March 2022 / Published online: 26 March 2022


## Abstract

A rapid and convenient fluorescence glyphosate (GLYP) biosensor was developed based on DNA-templated copper nanoparticles (DNA-CuNPs). In the absence of GLYP, the DNA-CuNPs were formed through the reduction of $Cu^{2+}$ by vitamin C (Vc). The DNA-CuNPs emitted intense fluorescence at 615 nm when being excited at 340 nm. In the presence of GLYP, GLYP can strongly chelate with $Cu^{2+}$ by the phosphate and carboxyl groups to decrease the amount of free $Cu^{2+}$. Due to the lack of free $Cu^{2+}$, DNA-CuNPs cannot be formed, which caused the fluorescence to decrease. The whole detection process of this proposed GLYP biosensor can be completed within 14 min. Titration experiments showed that this biosensor had a linear relationship for GLYP in the range 1 to 18 μM with a limit of detection (LOD) of 0.47 μM. This biosensor showed obvious selectivity among other pesticides, even between GLYP and organophosphorus pesticides. This biosensor performed well for GLYP detection in real samples with recoveries of 88.0–104.0%.

**Keywords** Glyphosate · Copper nanoparticles · DNA · Rapid detection

## Introduction

GLYP, a commonly used herbicide, can effectively and quickly remove weeds in the field. About 825,000 tons of GLYP was used worldwide in 2014 [1]. With the expansion of planting area, this number is expected to reach about 100 million tons in 2023 [2]. In China, the consumption of GLYP shows a rising trend as paraquat (another herbicide) is banned [3]. With the use of GLYP, many GLYP residues are found in soil and agricultural products. Unfortunately, GLYP can cause a variety of diseases and harm people's health. For example, it can lead to the growth delay of children [4], kidney damage [5], liver swelling, and steatohepatitis [6]. The maximum residue of GLYP was defined 0.7 μg $mL^{-1}$ (4.14 μM) in drink water by the U.S. Environmental Protection Agency (EPA) [7]. Therefore, it was necessary to develop a convenient and accurate analytical method for detecting GLYP.

Up to now, many methods and techniques have been designed to detect GLYP [8]. Traditional methods were mainly instrumental analysis, such as high-performance liquid chromatography (HPLC) [9] and gas chromatography (GC) [10]. These methods can achieve high sensitivity and reliability. However, they required a complicated derivatization process, because GLYP itself had no chromophores. Recently, a number of detection methods have been developed to overcome the above problems. These methods included immunoassay [11], enzymatic inhibition approaches [12], electrochemical sensors [13], metal–organic framework methods [14], and small chemical molecule methods [15, 16]. However, these methods

Huajuan Fang and Xingping Zhang contributed equally to this work.

✉ Hualin Yang
yanghualin2005@126.com

✉ Yu Zhou
zhouyurunye@sina.com

[1] College of Life Science, Yangtze University, 266 Jingmi Road, Jingzhou 434025, Hubei, China

[2] State Key Laboratory of Coordination Chemistry, Chemistry and Biomedicine Innovation Center (ChemBIC), School of Chemistry and Chemical Engineering, Nanjing University, Nanjing, China

[3] State Environmental Protection Key Laboratory of Synergetic Control and Joint Remediation for Soil &Water Pollution, Chengdu University of Technology, Chengdu 610059, Sichuan, China

[4] College of Animal Science, Yangtze University, 266 Jingmi Road, Jingzhou 434025, Hubei, China

suffered from difficult preparation of antibodies, complicated material synthesis, and long detection time. Therefore, a fast, simple, and convenient method is now highly advantageous.

In recent years, DNA-templated copper nanoparticles (DNA-CuNPs) have attracted great research interest as an excellent fluorescence material [17]. The DNA-CuNPs were first synthesized with double-stranded DNA (dsDNA) as templates by Mokhir group [18]. Then, the single-stranded poly T DNA was employed to synthesize poly T-CuNPs by Qing et al. [19]. Subsequently, dsDNA-CuNPs with ds(AT)n as template which had a better fluorescence efficiency were found by Wang group and Ouyang group [20, 21]. The mechanism of DNA-CuNPs formation was that DNA can promote the reduction of $Cu^{2+}$ and accumulate Cu(0) clusters to localize on the major groove of DNA [21]. Compared with other fluorescence nanomaterials, DNA-CuNPs exhibited many advantages including mild synthetic condition, cheap material, simple and rapid preparation, excellent photo stability, large Stokes shift, and low biological toxicity [17, 22]. With these advantages, DNA-CuNPs as a label-free reporter were widely used in the detection of targets such as $Cu^{2+}$ [23], ALP [24], and ATP [25]. However, to the best of our knowledge, DNA-CuNPs have not been used for the detection of GLYP. Inspired by the advantages of DNA-CuNPs, a fast, simple GLYP biosensor was designed in this work.

## Materials and methods

### Chemicals and materials

GLYP, vitamin C (Vc), glycine (GLY), and $CuCl_2$ were purchased from Sinopharm Chemical Reagent Co., Ltd. (Beijing, China; www.sinoreagent.com). Glufsinate (GLUF), aminomethylphylphonic (AMPA), temephos (TEM), dichlorvos (DDV), methamidophos (MDP), phoxim (PHO), carbendazim (CBZ), difenoconazole (DIF), jinggangmycin (JGM), thiamethoxam (TMX), uniconazole thiophanatemethy (TM), uniconazole (UN), oryzalin (OZ), trifluralin (TFL), and acetamiprid (ACE) were purchased from Yancheng Limin Agrochemical Co., Ltd (Yancheng, China; www.chinapesticides.com). The oligonucleotide DNA purified by PAGE was obtained from Shanghai Sangon Biological Engineering Technology & Services Co., Ltd (Shanghai, China; www.sangon.com). The DNA sequences was 5′- $(AT)_{30}$ -3′ from Ouyang's report which was described as polyAT-templated CuNCs showing higher fluorescence [21]. All reagents in this experiment were of analytical grade or above. All aqueous solutions were prepared with ultrapure water (18.2 MΩ cm) which was obtained from a Milli-Q water purification system.

### Fluorescence intensity analysis

All fluorescence measurements were performed on SpectraMax iD3 Multi-Mode Micropate Reader (USA). The instrument settings were as follows: $\lambda_{EX} = 340$ nm, $\lambda_{EM}$ from 550 to 700 nm. DNA-CuNPs were synthesized by simply mixing DNA, $Cu^{2+}$, and Vc. Firstly, 500 nM DNA and 35 μM $Cu^{2+}$ were added into 10 mM 3-(*N*-morpholino) propane sulfonic acid (MOPS) buffer (pH 7.6) containing 150 mM NaCl. Then, 2 mM Vc was added to reduce $Cu^{2+}$. After the mixture was incubated for 4 min at room temperature, the DNA-CuNPs formed and the fluorescence of DNA-CuNPs were measured in a microplate reader.

For GLYP titration experiment, the different concentrations (0, 1, 3, 5, 7, 10, 12, 15, 18, 21, 24, 27, 30 μM) of GLYP and 35 μM $Cu^{2+}$ were mixed first to react 10 min at room temperature. Then, 500 nM DNA and 2 mM Vc were added and incubated for 4 min. Lastly, the fluorescence was measured. The changes of fluorescence intensity were calculated by $(F/F_0) \times 100\%$. $F$ and $F_0$ were the fluorescence intensity in the presence and absence of GLYP, respectively.

The selectivity for GLYP was checked by comparing GLYP and other interferential substances under the same concentration (18 μM). The interferential substances included GLUF, AMPA, TEM, DDV, MDP, PHO, GLY, CBZ, DIF, JGM, TMX, TM, UN, OZ, TFL, and ACE. The interference experiments were studied by comparing the $F/F_0$ values before and after the addition of GLYP to the pesticide mixture containing other OPPs or other pesticides. The procedure was similar with the GLYP titration experiment.

### Ultraviolet and visible (UV–Vis) absorption

The UV–Vis absorption assay was performed on Model UH5300 Spectrophtometer Reader (Japan). The UV–Vis absorption between 260 and 500 nm was set for different treatment samples. The treatment conditions included (a) DNA + $Cu^{2+}$ + GLYP + Vc; (b) DNA + $Cu^{2+}$ + Vc; (c) DNA + GLYP + Vc; (d) DNA + $Cu^{2+}$ + GLYP; and (e) $Cu^{2+}$ + GLYP + Vc. The concentrations of DNA, $Cu^{2+}$, GLYP, and Vc were 500 nM, 35 μM, 50 μM, and 2 mM, respectively.

### Detection of GLYP in real samples

The agricultural products (rice, maize, and wheat) were purchased from a local farm product market in Jingzhou, Hubei province, China. Samples were pretreated according to the reported literature [26]. Initially, each food sample (1 g, rice, maize, or wheat) was mixed with 20 mL water. Then,

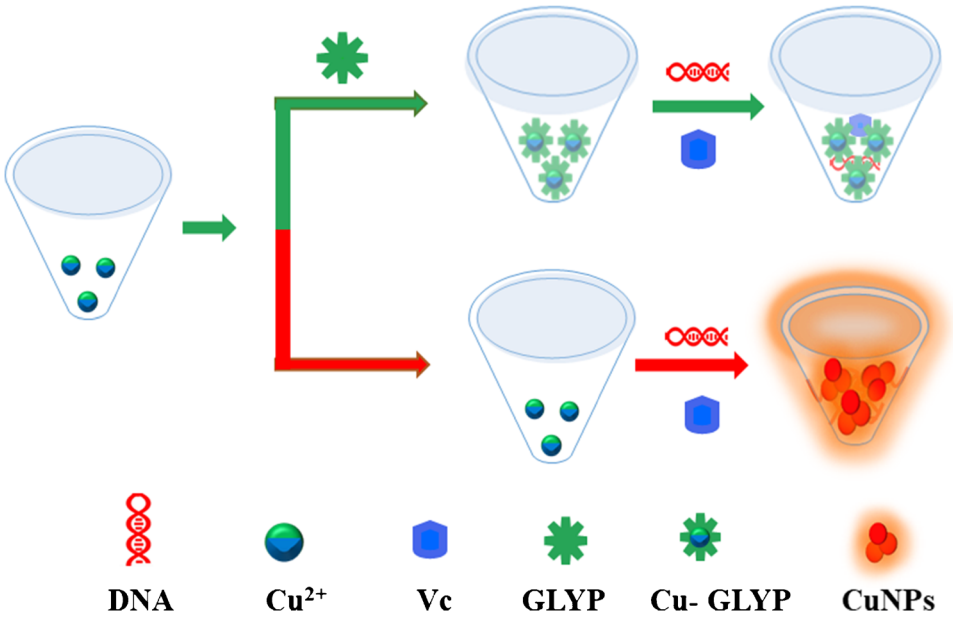


**Scheme 1** The principle of the proposed GLYP biosensor based on DNA-CuNPs

10 mL of dichloromethane was added and the mixture was sonicated for 15 min. Centrifugation followed for 10 min at 4500 rpm and the supernatant was collected. Subsequently, the supernatant was filtered by gauze. Then, the filtrate was evaporated to 2 mL left. Finally, different concentrations of GLYP (0–30 μM) were added to these samples, and GLYP was detected by the proposed method.

The water samples were collected in the campus pond of Yangtze University, rice field of Jingzhou City, and Yangtze River Jingzhou Section. Subsequently, the water samples were simply filtered by gauze to remove large particulate impurities. Then, the water samples were treated by adding different concentrations of GLYP (0–30 μM). Meanwhile, water samples without adding GLYP were used as control.

## Results and discussion

### The principle of the proposed GLYP biosensor

The principle of the proposed GLYP biosensor is illustrated in Scheme 1. The ds$(AT)_{30}$, $Cu^{2+}$, and Vc are employed to synthesize DNA-CuNPs. In this synthesis system, Vc is used as a reducing agent to reduce $Cu^{2+}$ to Cu(0). The dsDNA as a scaffold can template the formation of fluorescent CuNPs through promoting reduction of $Cu^{2+}$ and accumulating Cu(0) clusters to localize on the major groove of DNA [17, 21]. GLYP, containing functional groups of carboxyl (-COOH), imino (-NH-), and phosphonyl (-$PO_3H_2$), can strongly chelate with $Cu^{2+}$ to decrease the amount of free $Cu^{2+}$ [27–29]. Due to lack of free $Cu^{2+}$, the formation of DNA-CuNPs is prevented. Thus, in the absence of GLYP, the DNA-CuNPs can be formed to emit intense fluorescence. In the presence of GLYP, the DNA-CuNPs cannot be formed due to the chelation of GLYP and $Cu^{2+}$. As a result, the fluorescence decreases with the addition of GLYP.

### The feasibility of the proposed GLYP biosensor

The feasibility of the proposed GLYP biosensor was carried under different treatment conditions. The results are shown in Fig. 1A. Only mixing DNA, $Cu^{2+}$, and Vc, the fluorescence can be observed that suggested the DNA-CuNPs are formed (curve b in Fig. 1A). When any one of the three components (DNA, $Cu^{2+}$, or Vc) is removed, the fluorescence disappeared, which indicates that the DNA-CuNPs cannot be formed (curves c, d, and e in Fig. 1A). The fluorescence is completely disappeared when the GLYP is added, even DNA, $Cu^{2+}$, and Vc all exist (curve a in Fig. 1A). Meanwhile, the corresponding fluorescence photographs are recorded under UV irradiation. Only when DNA, $Cu^{2+}$, and Vc are present, a bright image can be observed (inset in Fig. 1A). This result implies that the proposed GLYP biosensor can be used to detect GLYP.

The UV–Vis absorption was used to further confirm the feasibility. When the DNA, $Cu^{2+}$, and Vc are mixed, a strong UV–Vis absorption can be observed at 350 nm due to the formation of DNA-CuNPs (curve b in Fig. 1B). When GLYP is added, the intensity of UV–Vis absorption decreases significantly (curve a in Fig. 1B). This result suggests that some of the DNA-CuNPs are destroyed. In the absence of DNA, $Cu^{2+}$, or Vc, almost no UV–Vis absorption is observed, which suggests no DNA-CuNPs are formed. The above results further verify the feasibility of the proposed GLYP biosensor.

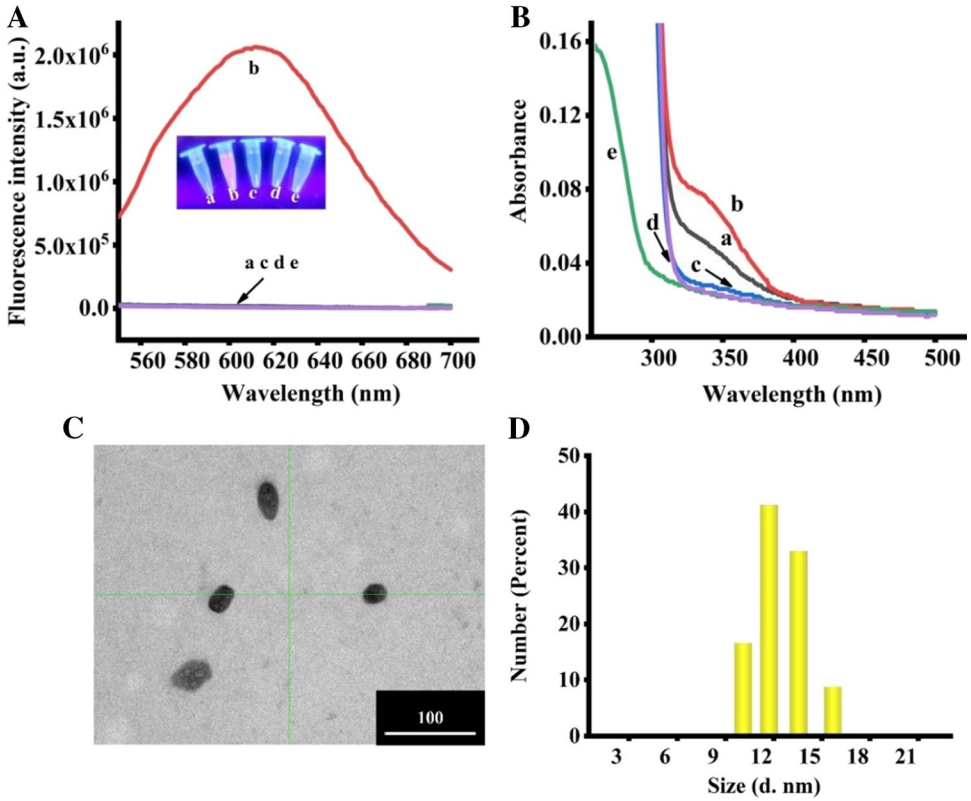


**Fig. 1** **A** Fluorescence spectra and (**B**) UV–Vis absorption under different treatment conditions. (**a**) DNA + $Cu^{2+}$ + GLYP + Vc; (**b**) DNA + $Cu^{2+}$ + Vc; (**c**) DNA + GLYP + Vc; (**d**) DNA + $Cu^{2+}$ + GLYP; (**e**) $Cu^{2+}$ + GLYP + Vc. The concentrations of DNA, $Cu^{2+}$, GLYP, and Vc were 500 nM, 35 μM, 50 μM, and 2 mM, respectively. Inset of (**A**): the corresponding fluorescence photographs ($\lambda_{EX}$ = 360 nm). (**C**) TEM images of DNA-CuNPs. (**D**) The particle size distribution diagram

Meanwhile, the result of fluorescence spectra and UV–Vis absorption also indirectly testifies the formation of DNA-CuNPs. Subsequently, transmission electron microscopy (TEM) is used to characterize the DNA-CuNPs as direct evidence (Fig. 1C). Dynamic light scattering (DLS) shows that the average diameter of DNA-CuNPs is about 12 nm which is consistent with the reported results (Fig. 1D) [30, 31].

## Optimization of detection conditions

The concentration of $Cu^{2+}$ was optimized by observing the fluorescence change of DNA-CuNPs under different $Cu^{2+}$ concentrations (Figure S1 A). Then, 35 μM $Cu^{2+}$ was chosen as an optimal concentration with the maximum fluorescence intensity. The concentration of Vc was optimized by Vc titration experiment. The results show that the fluorescence intensity stops rising and reaches a plateau when Vc increases to 2 mM (Figure S1 B). Thus, 2 mM Vc is used for the followed experiments.

For the detection time, the proposed GLYP biosensor can be distributed in two parts. One part is the reaction between GLYP and $Cu^{2+}$, and the other part is the formation of DNA-CuNPs. The results suggest that the DNA-CuNPs form very quickly in just 4 min (Figure S1 C) and GLYP reacts with $Cu^{2+}$ in 10 min (Figure S1 D). Thus, the whole detection process of this proposed GLYP biosensor can complete within 14 min.

## Sensitivity of the proposed GLYP biosensor

The sensitivity was researched by GLYP titration experiment. As shown in Fig. 2A, when the GLYP concentration is only 1 μM, the peak fluorescence signal at 615 nm had shown a significant change (from $2.75 \times 10^6$ to $2.61 \times 10^6$). As the GLYP concentration reaches 30 μM, the fluorescence is completely quenched. For quantitative analysis, the fluorescence peak value at 615 nm is studied. In the range of 0 to 30 μM, the calibration curve between GLYP concentrations and fluorescence changes fits a dose–response curve (Fig. 2B). The fluorescence changes show a linear relationship in the GLYP concentration range of 1 to 18 μM. The linear equation is $Y = 103.28 - 4.56\,X$ ($R^2 = 0.998$), where $Y$ and $X$ represent the fluorescence changes and GLYP concentrations (inset of Fig. 2B). The limit of detection (LOD) is estimated to be 0.47 μM based on three times standard deviation of blank samples. This LOD is lower than the maximum residue of GLYP (4.14 μM) in drink water defined by EPA [7]. Thus, the proposed GLYP biosensor has the potential to detect actual samples.

Subsequently, the proposed GLYP biosensor is compared with the reported methods (Table 1). The detection limit of this biosensor is better than or comparable

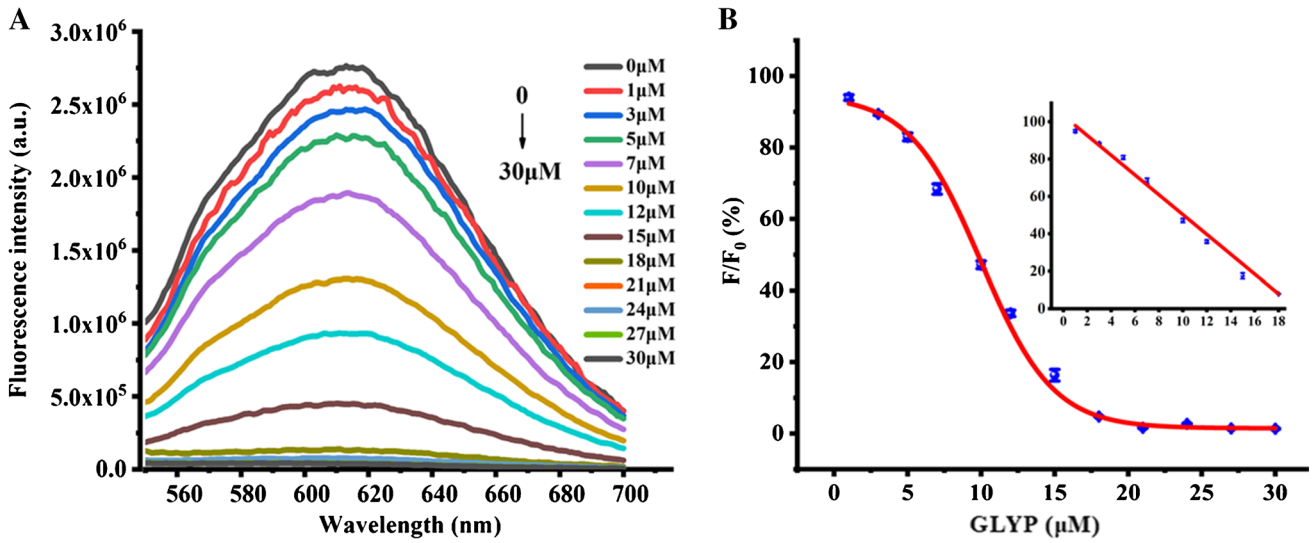


**Fig. 2** **A** Fluorescence spectra in different concentrations of GLYP. (**B**) The changes of fluorescence intensity at 615 nm under different GLYP concentrations. *F* and $F_0$ were the fluorescence intensity at 615 nm in the presence and absence of GLYP, respectively. Inset: fluorescence intensity and the concentration of GLYP showed a linear relationship between 1 and 18 μM range. The error bar represented the relative standard deviation of three repeated measurements

**Table 1** An overview on reported methods for the determination of GLYP

| Materials used | Material preparation | Linearity (μM) | Detection limit (μM) | Detection time (min) | References |
|---|---|---|---|---|---|
| $MoS_2$ nanosheets | Need | 2.36–11.8 | 0.51 | 30 | [32] |
| Carbon dots | Need | 0.02–2 | 0.6 | Not found | [33] |
| Au-Pt NPs | Need | 0.06–5920 | 0.03 | 70 | [34] |
| N-SiQD | Need | 0.59–5.92 | 0.043 | 6 | [28] |
| Carbon dots | Need | 0.18–59 | 0.09 | 24 | [35] |
| NaGdF4:Yb,Er (UCNPs) | Need | 0.29–739.3 | 0.05 | 60 | [29] |
| NaGdF4:Yb,Er (UCNPs) | Need | 29.6–739.3 | 5.9 | 60 | [29] |
| $Cu^{2+}$ | No need | 2–200 | 1.0 | 25 | [36] |
| HPLC | Need | 29.5–591.5 | 0.39 | Not found | [37] |
| HPLC | Need | 0.029–2.96 | 0.059 | Not found | [9] |
| DNA-CuNPs | No need | 1–18 | 0.47 | 14 | This work |

with the values obtained by other methods. Because this biosensor is carried out during the synthesis of DNA-CuNPs, it does not require preparation of nanomaterials in advance. Compared with other methods, the detection time of this biosensor is relatively short, which is a big remarkable highlight. Besides, the proposed biosensor has also been compared with the gold standard method (HPLC). In sensitivity, our method has no advantage over HPLC. However, HPLC requires a complicated derivatization process, because GLYP itself has no chromophores. Thus, our method is relatively simple.

## Selectivity and interference of the proposed GLYP biosensor

Selectivity and interference were evaluated as important indicators of detection methods. Firstly, seven common organophosphorus pesticides (OPPs) (GLUF, AMPA, TEM, DDV, MDP, PHO, and GLYP) and GLY (analog of GLYP) were employed to observe the response of the proposed biosensor. The structural formulas of these OPPs are showed in Figure S2. The results show that only GLYP causes a dramatic fluorescence change whereas other OPPs are at blank

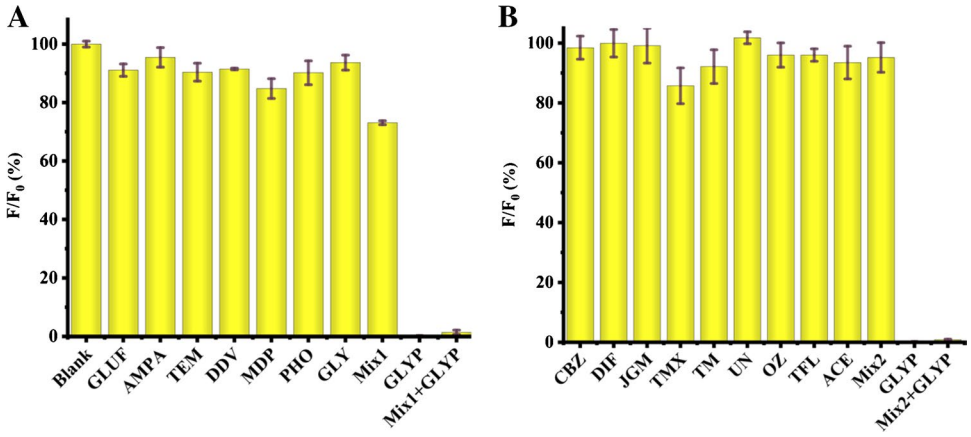


**Fig. 3** The selectivity and interference of the proposed GLYP biosensor for (**A**) organophosphorus pesticides (OPPs) and (**B**) other pesticides. The Mix-1 contained GLUF, AMPA, TEM, DDV, MDP, PHO, and GLY. The Mix-2 contained CBZ, DIF, JGM, TMX, TM, UN, OZ, TFL, and ACE. All interferential substances concentrations were 18 μM. The error bar represented the relative standard deviation of three repeated measurements

levels (Fig. 3A). The interference of other OPPs is studied by comparing the $F/F_0$ values before and after the addition of GLYP to mixture 1 containing other OPPs. The results show that the mixture of other OPPs still does not cause fluorescence changes. However, when GLYP is added, the significant fluorescence changes are observed again (Fig. 3A). Subsequently, the selectivity and interference of other pesticides for this biosensor were also studied. In this experiment, nine common other pesticides including CBZ, DIF, JGM, TMX, TM, UN, OZ, TFL, and ACE were employed. The structural formulas of these pesticides are showed in Figure S3. The results show that there is an almost 100% fluorescence quenching for GLYP and little change in other pesticides (Fig. 3B). The interference experiments also show that other pesticides do not interfere with the GLYP detection by comparing the $F/F_0$ values before and after the addition of GLYP to mixture 2 containing other pesticides (Fig. 3B). Besides, inorganic phosphates such as phosphate, hydrogen phosphate, and pyrophosphate have been employed to study the selectivity of this biosensor. The results show that inorganic phosphates do not affect the detection of glyphosate (Figure S4). These results suggest that the proposed GLYP biosensor has good selectivity for GLYP.

The reason of high selectivity is that GLYP and DNA (contained many phosphate groups) compete to bind $Cu^{2+}$. The GLYP and $Cu^{2+}$ can form stronger coordination compounds by three functional groups of carboxyl (-COOH), imino (-NH-), and phosphonyl (-$PO_3H_2$) with a high stability constant (lg $K = 11.92$) [27, 38]. The molecular structure of GLYP-$Cu^{2+}$ is showed in Figure S5. In the absence of carboxyl (-COOH) or imino (-NH-), the stability constant of GLYP decreases substantially by comparing the stability constants of glyphosate with its analogs (Table S1). Meanwhile, the stability constant of GLYP is much greater than that of inorganic phosphates (Table S1). Besides, the coordination ability of ppGpp-$Cu^{2+}$ whuch is stronger than that of pyrophosphate and phosphate and the coordination ability which is related to the number of phosphate have been reported [39]. Because DNA has a lot of phosphate groups, DNA has very high coordination ability for $Cu^{2+}$ which is stronger than that of inorganic phosphates. The high affinity of DNA ensures that other organophosphorus pesticides cannot compete with $Cu^{2+}$ to destroy DNA-CuNPs. Thus, the interference of other organophosphorus pesticides is avoided.

## Detection of GLYP in real samples

In order to study the reliability and potential application of the proposed GLYP biosensor, the GLYP in agricultural products and water samples were measured. For agricultural products, rice, maize, and wheat were chosen as representatives. Firstly, standard curves were established by means of standard addition. The linear equations of rice, maize, and wheat are $Y = 103.0 - 6.25\ X$ ($R^2 = 0.993$), $Y = 100.62 - 4.66\ X$ ($R^2 = 0.992$), and $Y = 106.88 - 6.73\ X$ ($R^2 = 0.986$), respectively (Figure S6, S7, and S8). Then, the spiked samples

**Table 2** Recovery test of the proposed GLYP biosensor in agricultural products

| Samples | Added GLYP (μM) | Found (μM) Mean ± SD ($n = 5$) | Recovery (%) | CV (%) |
|---|---|---|---|---|
| Rice | 0 | Not determinable | – | – |
| | 5 | 4.8 ± 0.4 | 96.0 | 8.3 |
| | 10 | 10.4 ± 0.9 | 104.0 | 8.6 |
| | 15 | 14.2 ± 1.4 | 94.6 | 9.8 |
| Maize | 0 | Not determinable | – | – |
| | 5 | 4.4 ± 0.3 | 88.0 | 6.8 |
| | 10 | 10.2 ± 0.8 | 102.0 | 7.8 |
| | 15 | 14.9 ± 1.2 | 99.3 | 8.1 |
| Wheat | 0 | Not determinable | – | – |
| | 5 | 4.5 ± 0.4 | 90.0 | 8.9 |
| | 10 | 8.9 ± 0.7 | 89.0 | 7.9 |
| | 15 | 14.5 ± 1.4 | 96.7 | 9.7 |

were measured. The results show that the recovery rates are in the range of 88.0–104.0% and the coefficient of variation is less than 15% (Table 2). For water samples, the linear equation in Fig. 2 is used. By calculating the GLYP concentrations in water samples, the recovery rates are from 92.2 to 107.9% (Table S2). And the coefficients of variation are all less than 15%. These results suggest our new method has potential application value for detecting GLYP in real samples.

## Conclusion

A rapid and convenient GLYP biosensor was developed based on DNA-CuNPs and the coordination of GLYP and $Cu^{2+}$. This biosensor was carried out during the synthesis of DNA-CuNPs. It did not require preparation of nanomaterials in advance. Most of the other methods were performed after the nanoparticles were synthesized [39]. Compared with other methods, the detection time of this biosensor was relatively short. Because the principle of this biosensor was that the GLYP and DNA (contained many phosphate groups) compete to bind $Cu^{2+}$, the high coordination ability of DNA for $Cu^{2+}$ guaranteed the high selectivity of this biosensor. This biosensor also performed well for GLYP detection in agricultural products and water samples which suggested this biosensor had great potential applications for detecting GLYP in practical samples. The idea of using the reaction between raw material of nanoparticles and target to achieve the purpose of detection provided a new way for the development of detection methods. In this biosensor, DNA-CuNPs were used as signal reporter with an excitation wavelength of 340 nm and an emission wavelength of 615 nm which cannot be visible to the naked eye. Thus, this method required a fluorescence detector. The development of visible biosensor to achieve in situ detection will be a future research direction.

**Supplementary Information** The online version contains supplementary material available at https://doi.org/10.1007/s00604-022-05284-8.

**Funding** The work is supported by the National Natural Science Foundation of China (31601536, 31871888), and State Environmental Protection Key Laboratory of Synergetic Control and Joint Remediation for Soil & Water Pollution (GHBK-2020–001).

## Declarations

**Competing interests** The authors declare no competing interests.

## References

1. Soukup ST, Merz B, Bub A, Hoffmann I, Watzl B, Steinberg P, Kulling SE (2020) Glyphosate and AMPA levels in human urine samples and their correlation with food consumption: results of the cross-sectional KarMeN study in Germany. Arch Toxicol 94:1575–1584
2. Parlapiano I, Biandolino F, Grattagliano A, Ruscito A, Libralato G, Prato E (2021) Effects of commercial formulations of glyphosate on marine crustaceans and implications for risk assessment under temperature changes. Ecotoxicol Environ Saf 213:112068
3. Tsai WT (2019) Trends in the use of glyphosate herbicide and its relevant regulations in Taiwan: a water contaminant of increasing concern. Toxics 7:4
4. Bailey DC, Todt CE, Burchfield SL, Pressley AS, Denney RD, Snapp IB, Negga R, Traynor WL (2018) Chronic exposure to a glyphosate-containing pesticide leads to mitochondrial dysfunction and increased reactive oxygen species production in Caenorhabditis elegans. Environ Toxicol Phar 57:46–52
5. Gunatilake S, Seneff S, Orlando L (2019) Glyphosate's synergistic toxicity in combination with other factors as a cause of chronic kidney disease of unknown origin. Int J Environ Res Public Health 16:2734
6. Mills PJ, Caussy C, Loomba R (2020) Glyphosate excretion is associated with steatohepatitis and advanced liver fibrosis in patients with fatty liver disease. Clin Gastroenterol Hepatol 18:741–743
7. Guan JP, Yang J, Zhang Y, Zhang XX, Deng HJ, Xu J, Wang JY, Yuan MS (2021) Employing a fluorescent and colorimetric picolyl-functionalized rhodamine for the detection of glyphosate pesticide. Talanta 224:121834
8. Valle AL, Mello F, Alves-Balvedi RP, Rodrigues LP, Goulart LR (2018) Glyphosate detection: methods, needs and challenges. Environ Chem Lett 17:291–317
9. Sun L, Kong D, Gu W, Guo X, Tao W, Shan Z, Wang Y, Wang N (2017) Determination of glyphosate in soil/sludge by high performance liquid chromatography. J chromatogr A 1502:8–13
10. Zhang W, Feng Y, Ma L, An J, Zhang H, Cao M, Zhu H, Kang W, Lian K (2019) A method for determining glyphosate and its metabolite aminomethyl phosphonic acid by gas chromatography-flame photometric detection. J Chromatogr A 1589:116–121
11. Viirlaid E, Ilisson M, Kopanchuk S, Mäeorg U, Rinken A, Rinken T (2019) Immunoassay for rapid on-site detection of glyphosate herbicide. Environ Monit Assess 191:507
12. Ibarra Bouzada LME, Hernández SR, Kergaravat SV (2019) Glyphosate detection from commercial formulations: comparison of screening analytic methods based on enzymatic inhibition. Int J Environ Anal Chem 101:1821–1835
13. Bettazzi F, Romero Natale A, Torres E, Palchetti I (2018) Glyphosate determination by coupling an immuno-magnetic assay with electrochemical sensors. Sensors-Basel 18:2965
14. Tan C, Liu G, Li H, Cui Y, Liu Y (2020) Ultrathin two-dimensional metal-organic framework nanosheets-an emerging class of catalytic nanomaterials. Dalton Trans 49:11073–11084
15. Hou J, Wang X, Lan S, Zhang C, Hou C, He Q, Huo D (2020) A turn-on fluorescent sensor based on carbon dots from Sophora japonica leaves for the detection of glyphosate. Anal Methods 12:4130–4138
16. Gui M, Jiang J, Wang X, Yan Y, Li S, Xiao X, Liu T, Liu T, Feng Y (2017) Copper ion-mediated glyphosate detection with N-heterocycle based polyacetylene as a sensing platform. Sensor Actuat B-Chem 243:696–703
17. Qing Z, Bai A, Xing S, Zou Z, He X, Wang K, Yang R (2019) Progress in biosensor based on DNA-templated copper nanoparticles. Biosen Bioelectron 137:96–109
18. Rotaru A, Dutta S, Jentzsch E, Gothelf K, Mokhir A (2010) Selective dsDNA-templated formation of copper nanoparticles in solution. Angew Chem Int Ed Engl 49:5665–5667

19. Qing Z, He X, He D, Wang K, Xu F, Qing T, Yang X (2013) Poly(thymine)-templated selective formation of fluorescent copper nanoparticles. Ang Chem 52:9719–9722
20. Qing TP, Qing ZH, Mao ZG, He XX, Xu FZ, Wen L, He DG, Shi H, Wang KM (2014) dsDNA-templated fluorescent copper nanoparticles: poly(AT-TA)-dependent formation. Rsc Adv 4:61092–61095
21. Song Q, Shi Y, He D, Xu S, Ouyang J (2015) Sequence-dependent dsDNA-templated formation of fluorescent copper nanoparticles. Chem Eur J 21:2417–2422
22. Qing T, Zhang K, Qing Z, Wang X, Long C, Zhang P, Hu H, Feng B (2019) Recent progress in copper nanocluster-based fluorescent probing: a review. Microchim Acta 186:670
23. Qing Z, Mao Z, Qing T, He X, Zou Z, He D, Shi H, Huang J, Liu J, Wang K (2014) Visual and portable strategy for copper(II) detection based on a striplike poly(thymine)-caged and microwell-printed hydrogel. Anal Chem 86:11263–11268
24. Zhu Y, Liu X, Liu K, Bao X, Cheng S, Zhang L, Zhang Y, Zhang L, Cao F, Xing X (2020) Enhanced-assay of alkaline phosphatase based on polyAT dsDNA-templated copper nanoclusters. Microchem J 158:105165
25. Song Q, Wang R, Sun F, Chen H, Wang Z, Na N, Ouyang J (2017) A nuclease-assisted label-free aptasensor for fluorescence turn-on detection of ATP based on the in situ formation of copper nanoparticles. Biosensor Bioelectron 87:760–763
26. Qu F, Wang H, You JM (2020) Dual lanthanide-probe based on coordination polymer networks for ratiometric detection of glyphosate in food samples. Food Chem 323:126815
27. Sheals J, Persson P, Hedman B (2001) IR and EXAFS spectroscopic studies of glyphosate protonation and copper(II) complexes of glyphosate in aqueous solution. Inorg Chem 40:4302–4309
28. Wang X, Yang Y, Huo D, Ji Z, Ma Y, Yang M, Luo H, Luo X, Hou C, Lv J (2020) A turn-on fluorescent nanoprobe based on N-doped silicon quantum dots for rapid determination of glyphosate. Microchim Acta 187:341
29. Liu Z, Yang L, Sharma AS, Chen M, Chen Q (2019) A system composed of polyethylenimine-capped upconversion nanoparticles, copper(II), hydrogen peroxide and 3,3′,5,5′-tetramethylbenzidine for colorimetric and fluorometric determination of glyphosate. Microchim Acta 186:835
30. Jain S, Jain A, Kachhawah P, Devra V (2015) Synthesis and size control of copper nanoparticles and their catalytic application. T Nonferr Metal Soc 25:3995–4000
31. Xiong Y, Gao B, Wu KS, Wu YQ, Chai YJ, Huang XL, Xiong YH (2018) Fluorescence immunoassay based on the enzyme cleaving ss-DNA to regulate the synthesis of histone-ds-poly(AT) templated copper nanoparticles. Nanoscale 10:19890–19897
32. Chen Q, Chen H, Li Z, Pang J, Lin T, Guo L, Fu F (2017) Colorimetric sensing of glyphosate in environmental water based on peroxidase mimetic activity of MoS2 nanosheets. J Nanosci Nanotechnol 17:5730–5734
33. Yuan Y, Jiang J, Liu S, Yang J, Zhang H, Yan J, Hu X (2017) Fluorescent carbon dots for glyphosate determination based on fluorescence resonance energy transfer and logic gate operation. Sensor Actua B-Chem 242:545–553
34. Ma J, Feng G, Ying Y, Shao Y, She Y, Zheng L, Abd Ei-Aty AM, Wang J (2021) Sensitive SERS assay for glyphosate based on the prevention of l-cysteine inhibition of a Au-Pt nanozyme. Analyst 146:956–963
35. Wang L, Bi Y, Gao J, Li Y, Ding H, Ding L (2016) Carbon dots based turn-on fluorescent probes for the sensitive determination of glyphosate in environmental water samples. Rsc Adv 6:85820–85828
36. Chang Y, Zhang Z, Hao J, Yang W, Tang J (2016) A simple label free colorimetric method for glyphosate detection based on the inhibition of peroxidase-like activity of Cu(II). Sensor Actuat B-Chem 228:410–415
37. Fang F, Wei R, Liu X (2014) Novel pre-column derivatisation reagent for glyphosate by high-performance liquid chromatography and ultraviolet detection. Int J Environ Anal Chem 94:661–667
38. Madsen HEL, Christensen HH, Petersen CG (1978) Stability constants of copper(II), zinc, manganese(II), calcium, and magnesium complexes of N-(phosphonomethyl)glycine (glyphosate). Acta Chem Scand A 32:79–83
39. Zhang P, Wang Y, Chang Y, Xiong ZH, Huang CZ (2013) Highly selective detection of bacterial alarmone ppGpp with an off-on fluorescent probe of copper-mediated silver nanoclusters. Biosens Bioelectron 49:433–437